CCFE
CULHAM CENTRE FOR FUSION ENERGY

UK Atomic Energy Authority

UKAEA-CCFE-PR(19)23

E. Militello Asp, G. Corrigan, P. da Silva Aresta Belo, L. Garzotti, D.M. Harting, F. Köchl, V. Parail, M. Cavinato, A. Loarte, M. Romanelli, R. Sartori

ITER Fuelling Requirements and Scenario Development for H, He and DT Through JINTRAC Integrated Modelling

ITER Fuelling Requirements and Scenario Development for H, He and DT Through JINTRAC Integrated Modelling

E. Militello Asp, G. Corrigan, P. da Silva Aresta Belo, L. Garzotti, D.M. Harting, F. Köchl, V. Parail, M. Cavinato, A. Loarte, M. Romanelli, R. Sartori

This is a preprint of a paper submitted for publication in Nuclear Fusion

JINTRAC Integrated Simulations of ITER Scenarios including Fuelling and divertor power flux control for H, He and DT plasmas

E. Militello Asp[1], G. Corrigan[1], P. da Silva Aresta Belo[1], L. Garzotti[1], D.M. Harting[1], F. Köchl[2], V. Parail[1], M. Cavinato[4], A. Loarte[3], M. Romanelli[1] and R. Sartori[4]

[1]CCFE, Culham Science Centre, Abingdon, Oxon, OX14 3DB, UK

[2]Technical University Wien, 1020 Vienna, Austria

[3]ITER Organization, Route de Vinon-sur-Verdon, CS 90 046, 13067 St. Paul Lez Durance Cedex, France

[4]Fusion For Energy Joint Undertaking, Josep Pla 2, 08019, Barcelona, Spain

E-mail contact of main author: Elina.Militello.Asp@ukaea.uk

Abstract. We have modelled self-consistently the most efficient ways to fuel ITER Hydrogen (H), Helium (He) and Deuterium-Tritium (DT) plasmas with gas and/or pellet injection with the integrated core and 2D SOL/divertor suite of codes JINTRAC. As far as we are aware, for ITER this is the first time modelling of the entire plasma has been carried out to follow the plasma evolution from X-point formation, through L-mode, L-H transition, steady-state H-mode, H-L transition and current ramp-down. We gave attention to keeping within ITER operational limits, in particular maintaining the target power loads below 10MW/m^2 by Ne seeding or main gas rate.

For the Pre-Fusion Plasma Operation phase our aim was to develop robust scenarios, including those required for the commissioning of systems with plasma. Our simulations show that commissioning and operation of the ITER Neutral Beam (NB) system to full power should be possible in 15 MA/5.3T L-mode H plasmas with pellet fuelling and 20MW of ECRH. For He plasmas gas fuelling alone is enough to allow access to H-mode conditions at 7.5 MA/2.65T with 53-73 MW of additional heating, as after application of NB and during the ensuing L-H transition, the modelled density build-up quickly reduces the NB shine-through losses to acceptable levels. These He H-modes should allow the characterisation of ITER H-mode plasmas and the demonstration of ELM control schemes to take place in the non-active phase before ITER DT operation.

In ITER DT plasmas we have explored, by varying the fuelling and heating schemes, the best route to achieve the target fusion gain of Q=10 and how to exit the plasma from such conditions with acceptable divertor loads. The use of pellet fuelling in DT can provide a faster route to increase the density in L-modes, but it is not essential for unrestricted NB operation due to the lower shine-through losses compared to H. During the H-L transition and current ramp-down, gas fuelling and Ne seeding are required to keep the divertor power loads under the engineering limits but precise control over radiation is needed to prevent the plasma becoming thermally unstable.

1. Introduction

The ITER Research Plan **Error! Reference source not found.** foresees a sequence of plasma operational campaigns in hydrogen/helium, deuterium, and ultimately deuterium-tritium mixtures for the demonstration fusion power production. In the non-active operational phase (Pre-Fusion Plasma Operation) commissioning of the tokamak systems such as diagnostics, fuelling, heating and current drive systems, in vessel coils and plasma control systems will take place. Early operational experience and experimental results in Hydrogen (H), Helium (He), and then later in Deuterium (D) will also give insights on strategies to optimise Deuterium-Tritium (DT) plasma scenarios. This is important to ensure ITER's success in its primary goal of achieving high fusion performance. The plasma density profile and its evolution are known

to be very important in determining the best route to achieve the target fusion gain, Q=10, in ITER H-modes using the available additional heating [1].

In present devices gas puffing and recycling can efficiently fuel the core plasma as the edge plasma is fairly transparent to neutrals. In contrast, the ITER edge plasma will be hotter and denser so that hydrogenic neutrals will be ionised in the far scrape-off-layer (SOL) and will not penetrate to the separatrix[3][4][5][6]. Thus, pellet injection, even if its deposition is rather peripheral in ITER, will be required to fuel the core plasma in ITER.

So far ITER integrated plasma simulation studies of fuelling and particle transport in ITER scenarios have been performed by introducing the sources from the scrape-off layer through boundary conditions in core plasma modelling suites (e.g. [7]). Here, to our knowledge, for the first time, we report on simulations including coupled core-edge transport calculations that follow the entire ITER plasma discharge evolution from just after X-point formation. This modelling approach allows us to study and optimize the fuelling of the plasma and to adjust the additional heating waveforms in H, He and DT plasmas to achieve the required stationary plasma conditions while avoiding operational limits, e.g. excessive neutral beam (NB) shine-through loads on the first wall panels and divertor power fluxes (limited to 10MW/m^2 in ITER) to be exceeded.

For non-active H and He plasmas we carried out L-mode simulations to identify robust scenarios for which the density is sufficiently high to operate and commission the NB at maximum beam voltages with acceptable first wall loads; namely a line-average density of $4.5\text{x}10^{19}\text{m}^{-3}$ in H and $3.0\text{x}10^{19}\text{m}^{-3}$ in He[8]. It is important to note that for fuelling of H plasmas both H gas fuelling and pellet fuelling are available. For He plasmas only gas fuelling can be used to fuel He; it is possible to inject H pellets, but this can lead to He dilution and thus increase the density required to inject NB with acceptable shine-through first wall loads. In addition, the L-H power threshold also increases with the H dilution in He plasmas [9][10][11][12] and thus injecting H pellets into He plasmas can increase the required power to access the H-mode in the initial phase of ITER operation beyond the capabilities in this operational phase. Therefore, in our He plasmas simulations we have concentrated on gas fuelled plasmas as these are of highest relevant for the non-active operational phase where H-mode plasmas are expected to be explored first in ITER.

In our simulations of the 15MA/5.3T ITER baseline scenario plasmas with 50/50 DT composition, the main emphasis has been placed on the optimization of the fuelling and impurity seeding to achieve high Q operational conditions with acceptable power loads to the first wall and divertor. This requires a sufficient density to inject the full power NB during the L-mode phase and an optimized fuelling scheme after the plasma enters the H-mode phase. Previous studies have shown that an excessive density rise in the initial H-mode phase can decrease the core plasma temperature and prevent the fusion power build-up thus causing the return of the plasma to L-mode [13]. On the other hand, a too low plasma density in this phase can lead to the divertor power flux to exceed the design value of 10 MWm^{-2}. Therefore our H-mode access simulations have optimised the fuelling rate and impurity seeding rates to reach a robust H-mode in an as short time as possible with high fusion gain (Q ~ 5) and this is then followed by a higher fuelling rate in which the plasma density increases to ~ 85-90% of the Greenwald limit for which Q = 10 is expected to be achieved in ITER. Extensive fuelling optimisation studies for the stationary phases of ITER DT H-modes over a range of plasma currents and toroidal fields are described in [14]. While the control of the density and divertor power fluxes through divertor radiation by impurity seeding in the access to high Q operation requires some optimization, this is much more challenging for the exit phase of high Q operation. In this phase the plasma density decreases, and this can lead to a significant increase of the divertor power fluxes with values in excess of 10 MWm^{-2}. Careful adjustment of both

plasma fuelling (pellet and gas fuelling) and impurity (Ne) seeding is required to prevent excessive divertor power fluxes as well as the radiative collapse of the plasma solution in this phase due to excessive divertor radiation. This radiative collapse if reflected in our simulations by a numerical instability that corresponds to the experimental situation in which full plasma detachment takes place, possibly followed by a thermal instability such as a MARFE. Although in this paper we use the experimental terminology for this numerical instability, we do not and cannot model these physical phenomena in detail.

To model the above ITER plasma conditions and scenarios comprehensively and self-consistently, we have used the integrated suite of core and SOL/divertor transport codes JINTRAC [14] developed at JET. This suit couples JETTO/SANCO[16][17], a 1.5D core transport solver that includes impurities, with EDGE2D/EIRENE[18][19], a 2D SOL/edge multi-fluid solver that includes plasma interactions with the ITER Be wall and W divertor. For simplicity, the only impurities that we have modelled are Be and Ne.

In the initial phase of our ITER JINTRAC simulation studies, we carried out an extensive benchmark between EDGE2D and SOLPS 4.3 [20] in order to ensure that the SOL/divertor physics description was consistent between the two codes [21][22][23]. Moreover, we have also extensively modified EDGE2D to model plasmas with He as the majority species. In this paper we present what to our knowledge are the first fully integrated core-edge simulations of He plasmas, applied to ITER in this specific case. Another noteworthy consequence of this development work is that EDGE2D is now capable of handling plasmas with two main hydrogenic species, which is essential for the simulation of fuelling by gas puffing and recycling for DT plasmas.

The outline of the paper is as follows: in Section 2 we describe the JINTRAC modelling suite and our modelling assumptions. Our results for the simulations of ITER plasmas in the non-active phase are described in Section 3 and the simulations of DT plasmas in Section 4 with the summary and conclusions in Section 5.

2. JINTRAC Modelling Assumptions

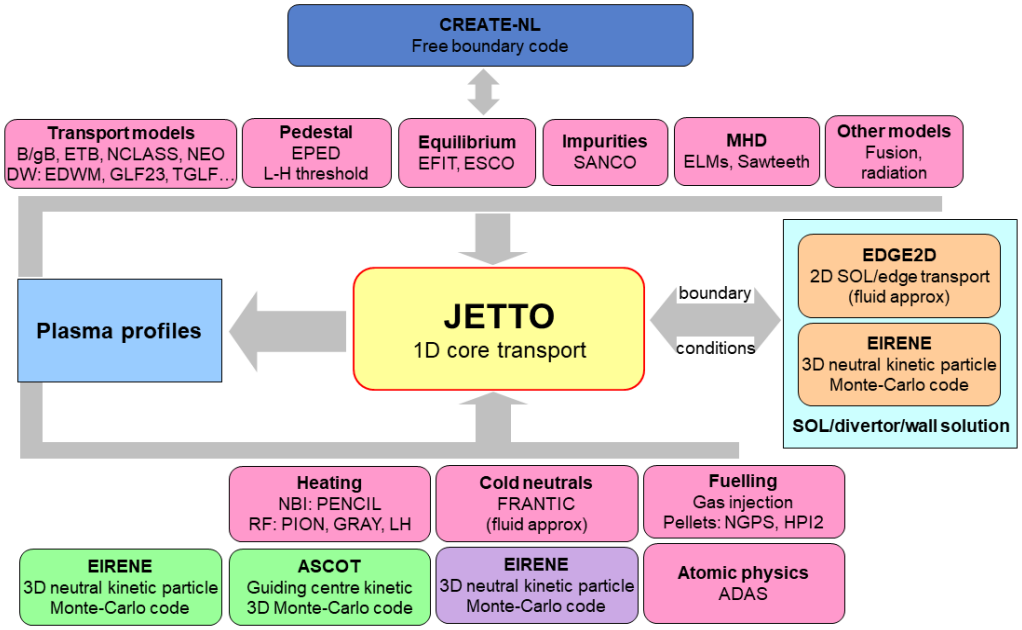

-

Figure 1. Schematic of the JINTRAC modelling suite

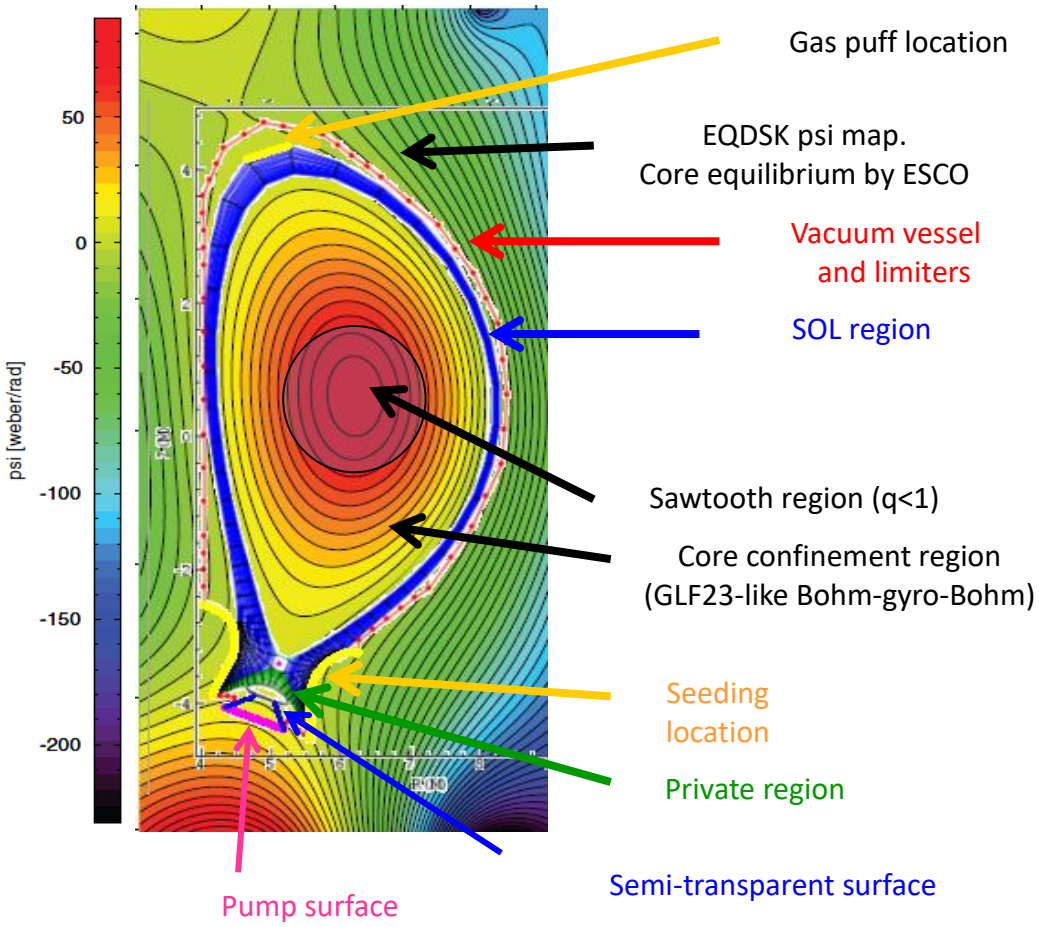

Figure 2. Poloidal magnetic flux (ψ) map of the MHD equilibrium for an ITER 15MA/5.3T plasma. Superimposed are the EDGE2D grid, the ITER first wall and the divertor target structure with dome, semi-transparent surfaces and pump.

The simulations that we present here follow most of the time evolution of the ITER DT and He H-mode reference plasma scenarios from the initial L-mode at X-point formation at low current through the build-up to the stationary ELMy H-mode phase, including the L-H transition, the initial ELM-free H-mode and, finally, the stationary ELMy H-mode phase with controlled ELMs. For DT plasmas we have also studied the H-L transitions, with particular emphasis on keeping the divertor power load and divertor plasma temperature under control. Generally, the main focus of the simulations in He and DT have been on the fuelling requirements to obtain an appropriate plasma density and to control its evolution for: 1) the unrestricted use of the NB in L-mode plasmas to trigger the L-H transition; 2) reaching and sustaining ELMy H-mode conditions; and 3) for 15 MA plasmas in DT, reaching a Greenwald density fraction of 85%, which is required to obtain the Q=10 ITER inductive goal. For H plasmas a set of dedicated studies was performed to evaluate the possibility of achieving the minimum density, which is required for the unrestricted use of the ITER NB at highest injection energy (870 keV for H neutrals), in L-mode plasmas. This is important for the use of the NB system in the initial phases of ITER operation; the required density is$4.3\text{x}10^{19}\text{m}^{-3}$ for H plasmas, which is considerably larger than for DT ($2.5\text{x}10^{19}\text{m}^{-3}$). Hence these simulations have been done at constant values of field and current rather than for the whole plasma scenario as done for the He and DT H-mode plasmas.

In the JINTRAC modelling suite (Figure 1. and Figure 2.) the core plasma is fuelled by gas fuelling (in our case through a gas inlet valve at the top of the machine), pellets (for H and DT

plasmas) injected from the high field side and by the several sources of recycled neutrals, as calculated by EDGE2D/EIRENE. These include neutrals recycled both at the Be main-chamber wall and W divertor targets.

It should be noted that in the present work we have assumed that recycled neutrals can only cool the plasma and therefore do not contribute significantly to the recycling of energy in the SOL/divertor. This is a sound assumption for recycling on Carbon or Beryllium plasma facing materials, where fast reflections (from an ion returning as an atom) are less probable than thermal reflections (where the ion returns as part of a molecule). In addition, with a Carbon wall the recycled power fluxes are also reduced by the formation of carbohydrate molecules and by the relatively high wall retention of hydrogenic species, which increases the power absorption of the wall. The lower retention in W walls and the small hydrogen to W mass ratio imply that fast reflections become more probable from a W wall, which increases the recycled energy flux. In Appendix A we present analysis of the impact of such effect by using a model that is more sophisticated in its description of the recycled energy flux from W than the one used in most of the studies in the paper. The assessment of Appendix A shows that there is a minor effect on the core and SOL plasma of the increased energy recycling coefficient whereas in the divertor this effect is more significant and makes the divertor less detached for given upstream plasma conditions in the SOL.

Contrary to existing tokamaks, the high recycling regime in ITER (i.e. a much larger divertor flux than the outflux from the core plasma) persists even at low separatrix densities and high divertor temperatures [24], due to the large divertor plasma dimensions which lead to a very efficient neutral ionisation. Hence, for most plasma conditions in ITER a clear majority of the recycled neutrals in ITER are ionised in the divertor plasma and, typically less than 1% of the total neutral recycling flux actually reaches the core plasma where it is ionised [5]. This makes fuelling of the plasma by gas fuelling and the ensuing increased recycling very ineffective to fuel the core plasma and to increase the core plasma density. Indeed, core plasma fuelling is foreseen to be performed by the injection of pellets in ITER. This is modelled with the modules NGPS [25] and HPI2[26], which are integrated in JETTO and describe the ablation and deposition of the pellet mass taking into account the post-ablation drift. As shown in Figure 2 the EDGE2D/EIRENE model includes a pump and stationary conditions are established when the neutral pumped flux is equal to the gas + pellet fuelling flux.

In addition to the modelling of the fuelling of ITER plasmas and the control of the density evolution, our simulations have also addressed the control of divertor power loads. In ITER operation it is required to maintain the divertor peak power flux below their design limit of $10MW/m^2$. For a range of plasma scenarios conditions (typically high power/high current plasmas) the achievement of this power flux level has required the introduction of Ne into the plasma, which has been modelled by a gas puff in the outer divertor target region. The resulting Ne radiation in the SOL/divertor can be very effective in reducing the power flux at the target and decrease the divertor plasma temperature, which is important to limit W sputtering.

For the lower power phases of the plasma scenarios (e.g. L-mode phases) we have frequently observed that injection of Ne was not required to achieve power fluxes under the ITER design limit; this could be achieved by increasing the edge plasma density by gas fuelling alone. On the other hand, in the phases where large SOL power fluxes occur together with a fast evolution of the edge plasma parameters (e.g. H-mode termination phases), it is extremely complex to adjust gas fuelling and Ne injection to maintain the divertor power flux under the design limit while avoiding a strong detachment of the divertor, which leads to numerical instabilities in the code. This is due to the strong coupling between core and edge plasma (e.g. through the edge power flux that determines the level of confinement which, in turn, is affected by the increased core plasma radiation from the injected Ne). In this paper we present first results of the control

of the divertor power fluxes in such phases, which has been achieved by manually tuning the gas fuelling and Ne injection level by trial and error. A more systematic study of power flux control in H-mode termination phases in ITER scenarios requires appropriate feedback loops for gas puffing and Ne injection to be implemented in JINTRAC; this work is in progress and will be used for future ITER simulations.

The simulations presented here consider a single isotopic specie in the SOL and divertor to represent D and T. At the separatrix the resulting ion density and neutral influx from EDGE2D is transferred to the core plasma model in JETTO as being composed of 50% D and 50% T. Conversely, the total DT plasma particle outflux crossing the separatrix from JETTO is converted into a single hydrogenic isotopic specie when transferred to EDGE2D. Successful core+SOL/divertor test simulations of JET DT plasmas have been carried out with a more recent version of EDGE2D, which can handle plasmas with two main hydrogenic species[21]. The results of this version will be benchmarked against JET Hydrogen-Deuterium experimental plasmas before using it predictively for ITER.

For the simulations presented here we have developed a special version [5] of the standard JETTO Bohm-gyro-Bohm transport model tuned to GLF23[27], which includes a collisionality dependent particle pinch that reproduces the density peaking seen in GLF23 associated with anomalous transport fluxes at low collisionalities. The transport of the impurities, Be sputtered from the main chamber wall and Ne seeding to keep the divertor power fluxes acceptable are described by SANCO for the core plasma assuming that their transport can be described by the linear combination of neoclassical transport and anomalous transport with the impurities having the same anomalous transport as the main ion species. We have used NCLASS [28] to calculate the neoclassical transport for all particle species (main ions and impurities).

Although we have evolved the core equilibrium in our simulations with ESCO, the internal fixed-boundary equilibrium solver in JETTO, for technical reason we had to keep the EDGE2D grid fixed in poloidal shape. Therefore, in our current ramp-up and ramp-down simulations the plasma poloidal shape is assumed to remain unchanged and we have adjusted the pitch of the magnetic field in the SOL to reproduce the change in connection length associated with the changes to the poloidal field as the plasma current varies during these phases.

The auxiliary heating schemes in the ITER baseline are radio frequency (RF) heating by ECRH (Electron Cyclotron Resonant Heating) and ICRF (Ion Cyclotron Radio Frequency Heating) and NB (neutral beam) injection, all of which we have used in the modelling. We have used PENCIL [29] to calculate the NB power deposition profiles in DT plasmas, and due to the limitations of PENCIL, we have used ASCOT[30] for He plasmas.

ITER considers a range of ICRF heating schemes which range from He^3 minority and second harmonic T at a toroidal field value of 5.3 T to H minority at 2.65 T for He plasmas. Although the module PION [31], included in JINTRAC, is, in principle, able to calculate the ICRF heating profiles, in the simulations presented here we have, for simplicity, assumed an ad-hoc Gaussian ICRF deposition profile centred on-axis with equal distribution of the power to the ions and electrons; this is a good approximation for DT plasmas at 5.3T while it overestimates slightly the core ion heating for H minority of He plasmas.

For ECRH heating we have also assumed an ad-hoc Gaussian power deposition centred at a normalised minor radius 0.2. The recent installation of GRAY [32] in JINTRAC would allow to calculate the ECRH heating and current drive self-consistently in future ITER studies. However, as the main aim of this study is to determine fuelling requirements for ITER scenarios and to investigate schemes for divertor power load control, the use of ad-hoc RF deposition profiles is an acceptable simplification.

As there currently is no first-principle model that can accurately predict confinement transitions, we have relied on experimental observations and scaling laws to determine the power level at which the plasma access or exits the H-mode confinement regime in ITER scenarios. We have applied the Martin L-H threshold scaling [33]

$$P_{LH} = 2.15e^{\pm 0.107} n_{e20}^{0.782\pm 0.035} B_T^{0.803\pm 0.032} S^{0.941\pm 0.019}$$

where P_{LH} is the threshold power in MW, n_{e20} the line-average density in 10^{20}m^{-3}, B_T the magnetic field in T, and S the plasma surface area in m^2. An L-H confinement transition is assumed to occur in our simulations when

$$P_{Loss} - P_{LH} \geq 0,$$

where P_{Loss}, the loss power crossing the separatrix is

$$P_{Loss} = P_{OHM} + P_{abs} - dW/dt - P_{Floss}$$

and P_{OHM} is the ohmic power, P_{abs} the absorbed power, W the total plasma energy and P_{Floss} is the fast ion losses. Conversely an H-L transition occurs in the simulations when $P_{Loss} - P_{LH} \leq 0$.

The Martin scaling was derived for deuterium plasmas. It has been observed in AUG, DIII-D, and JET[10][11][12] that for He plasmas the L-H transition threshold is higher by a factor of 1.44 than for D plasmas, a factor which we have used in our simulations of He L-H transitions.

The edge transport barrier (ETB) width has been determined with the EPED1 model [34] and we have assumed this value to remain fixed throughout the L-H and H-L transitions, i.e. whenever P_{Loss}-$P_{LH}\geq 0$. However, we allow the level of residual anomalous transport within ETB to depend on the excess of heat flux through the separatrix, P_{Loss}, with respect to power threshold P_{LH} so that for

$$P_{loss} - P_{LH} > 0$$

$$\chi, D_{ETB} = \chi, D_{anomolous} e^{-(P_{loss}-P_{LH})/(P_{LH}\cdot\Delta_{LH})} + \chi, D_{Ncoclassical},$$

where Δ_{LH} determines the rate of decay of the anomalous transport with the edge power flow margin over the power threshold. In line with experimental observations on JET we use Δ_{LH}=0.1 [35], which also allows for smoother transitions with less dithering between L- and H-mode.

Following the L-H transition the pressure in the ETB builds up and the ballooning stability parameter α rises. When it reaches a prescribed value, α_{crit}, evaluated on the basis of edge ideal MHD stability, we trigger the continuous ELM model. This consists of an ad hoc increase of transport in the ETB to maintain $\alpha = \alpha_{crit}$ throughout the stationary phase of the ELMy H-mode. This is an approximation to the expected plasma behaviour of ITER ELMy H-modes where ELM energy losses need to be controlled to very small values and on ELM suppression is foreseen [36].

Finally, we have used the Kadomtsev model [37] to calculate the sawtooth reconnection. A sawtooth crash is triggered when the safety factor is below unity at the magnetic axis but only after a set minimum time (0.1s) has passed since the last crash to avoid too frequent crashes destabilising the code. However, in most of our simulations sawtooth crashes normally occur much more infrequently than this.

3. JINTRAC Simulations of the Non-Active Phase of ITER operation (Pre-Fusion Plasma Operation)

We have focussed our non-active fuelling modelling studies on the achievement of appropriate L-mode densities in H ($4.3\text{x}10^{19}$m^{-3}) and He ($2.7\text{x}10^{19}$m^{-3}) to allow for unrestricted operation

and commissioning of the NB over the whole range of injected hydrogen ion energy (500-8700 keV) up to the highest values, and on the achievement of ELMy H-mode plasmas in He. Experimental evidence from several tokamaks for hydrogenic plasmas, such as JET [9], show that $P_{LH} \propto 1/A_{eff}$ where A_{eff} is the effective atomic mass and, hence, the threshold power for hydrogen plasmas is expected to be significantly higher than for DT. For ITER this implies that H H-modes are unlikely at heating powers below 100MW at full current and field. Therefore, H-mode studies in the non-active phase are expected to take place at reduced currents and fields and most likely in He to take advantage of the reduced power threshold compared to H plasmas ($P_{LH}^{H} = 1{,}4\ P_{LH}^{He} = 2\ P_{LH}^{D}$). Predictions for 7.5MA/2.65T H-modes in ITER show that the ELMs may produce energy loads above the melting limits for the W divertor monoblock target and, hence, such plasmas provide highly relevant conditions for the understanding of H-mode plasma behaviour in ITER and for the commissioning and refinement of the ELM control system to demonstrate that ITER can achieve the required level of ELM control before the start of nuclear operations **Error! Reference source not found.**.

3.1.Hydrogen L-mode Simulations of 15 MA/5.3 T plasmas

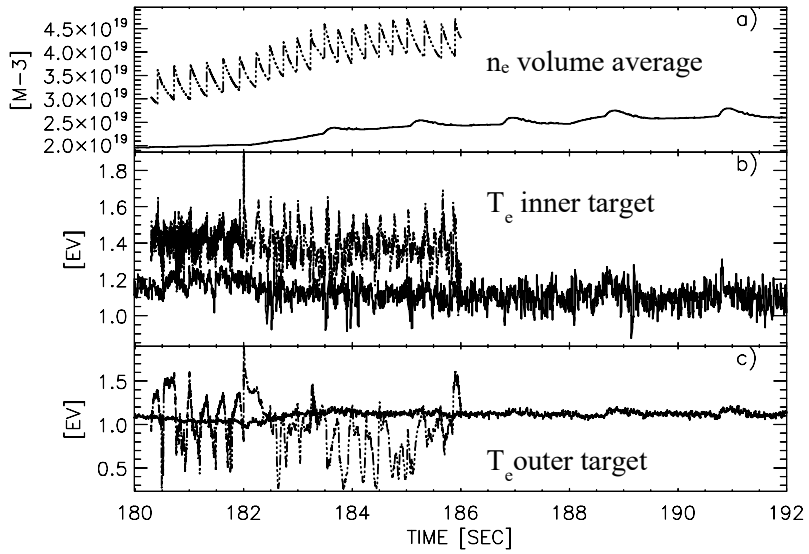

Figure 3. Integrated modelling of an ITER 15MA/5.3T H L mode plasma with gas fuelling $3.0x10^{22}$/s and 40MW of ECRH (solid); and pellet fuelling, $5.3x10^{21}$ particles/pellet at 3.3-4.0Hz (corresponding to a fuelling rate of ~ 10^{22}/s), with gas fuelling $5.0x10^{20}$/s and 20MW of ECRH (chain). The pellet causes oscillations in the target temperatures rendering the outer target transiently detached (T_e<1eV).

Our simulations of 10MA and 15MA hydrogen L-mode plasmas at 5.3T predict that gas fuelling alone will not be sufficient to reach the density of $4.3x10^{19}m^{-3}$ for unrestricted NBI operation, even when the plasmas are heated with the maximum baseline level of 40MW RF power. Indeed, for both currents we only reached line-average densities of up to ~ 2.8-$3.1x10^{19}m^{-3}$ for a gas rate between 2.5-$3.0x10^{22}s^{-1}$(Figure 3). For higher gas fuelling rates the divertor strongly detaches, which could lead to the triggering of radiation instabilities such as a MARFE, the separatrix density saturates and consequently the core density does not increase with gas fuelling beyond these rates.

To increase the density further, we have investigated fuelling of these plasmas with dominant pellet fuelling by reducing the gas rate to a very low value of $5.0x10^{20}s^{-1}$ and injecting pellets ($90mm^3/5.3x10^{21}$ particles) into the plasma. By applying an initial pellet frequency of 3.3Hz and then increase it to 4Hz after 4.5s, a 15 MA/5.3T hydrogen L-mode plasma can reach a line-average density of $\sim 4.6x10^{19}m^{-3}$ even when it is heated by only 20MW of ECRH (FigureFigure 3.). To ensure that this plasma remains thermally stable the gas fuelling needs to be kept at very low values. As a rule of thumb, target temperatures less than 1eV indicate a high level of detachment in our simulations and a likelihood of thermal instability of the solution. For these pellet-fuelled hydrogen plasmas, the inner target temperature remains above 1eV whereas the outer target temperature can temporarily decrease under this value due to the intermittent particle outflux from the plasma caused by injected pellet. It is important to note that these simulations do not contain extrinsic impurities such as Ne seeding because the divertor power loads remained well under 10 MWm^{-2}; the Be content was also very low in these simulations with $Z_{eff} \approx 1$ throughout the core and edge plasma in these simulations.

3.2. Simulation of He H-mode scenarios at 7.5 MA/2.65 T

We have performed simulations of ITER helium H-mode plasma 7.5 MA/ 2.65 T scenarios including the plasma current ramp-up and the access to stationary H-mode. The starting conditions correspond to a diverted He L-mode plasma at 3MA/2.65T with 20MW ECRH heating and a volume-average electron density of $1.0x10^{19}m^{-3}$; the modelled ramp-rate is 200kA/s leading to the flat top current being reached 22.5 s after X-point formation at 3 MA. To model the carrying current equilibrium the poloidal flux ψ has been rescaled with the increasing current and the edge field line pitch in the SOL adjusted correspondingly while maintaining a constant plasma shape. Different levels of gas puff have also been considered to investigate the resulting increase in density. From the results of the simulations it is clear that the density ramp rate during the current ramp-up is very sensitive to the prescribed level of gas puff. If the gas puff level is too high ($>6x10^{21}$ /s), it can cause early detachment of the divertor and thermal instability of the numerical solution, whereas if it is too low ($<1x10^{21}$ 1/s), the density cannot be increased together with the plasma current as required for the later access to H-mode in this scenario. To ensure the achievement of the required density we have implemented a numerical feedback scheme in the JINTRAC suite to adjust the level gas puff to provide a density ramp at fixed Greenwald fraction, which we have chosen to be ~ 50%.

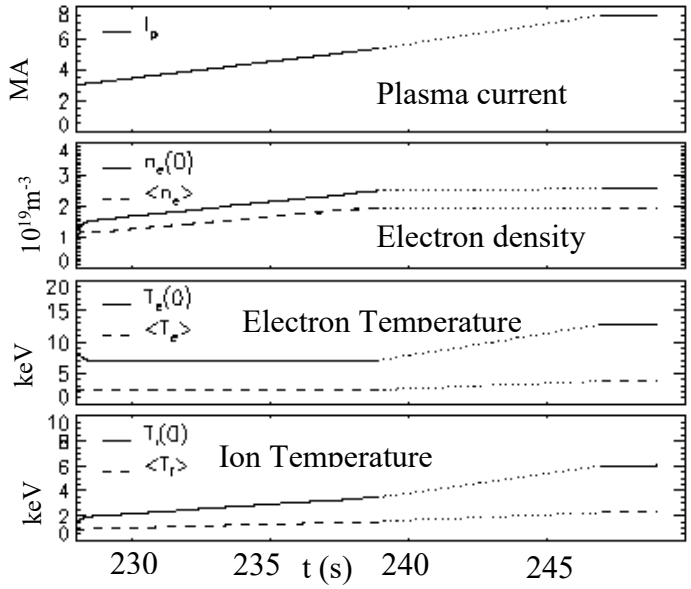

Figure 4. Simulation of a He H-mode plasma scenario with flat top current and field of 7.5 MA / 2.65 T from X-point formation at 3 MA / 2.65 T, 20MW ECRH. The first part of the solid (on-axis) and dashed (volume-average) lines shows the simulated ramp up to 5.5 MA, the second part shows the steady state target L-mode prior to NB injection at 7.5 MA. The dotted line shows the missing part of the simulation, which could not be completed as the inner divertor approached detachment.

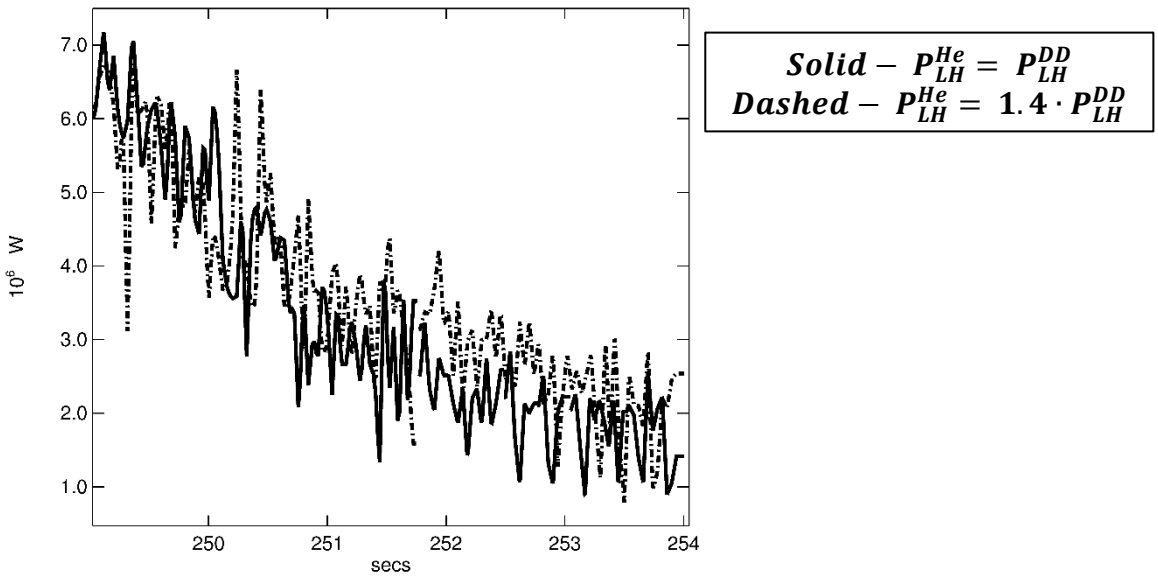

Figure 5. Neutral beam shine-through power as calculated by ASCOT for the L-H transition in 7.5MA/2.65T He ITER plasma with 33MW NB and 20MW ECRH. With both an optimistic (solid) and realistic (dashed) L-H power threshold for He plasmas compared to DD plasmas, the shine-through power decreases within 5 s to low values.

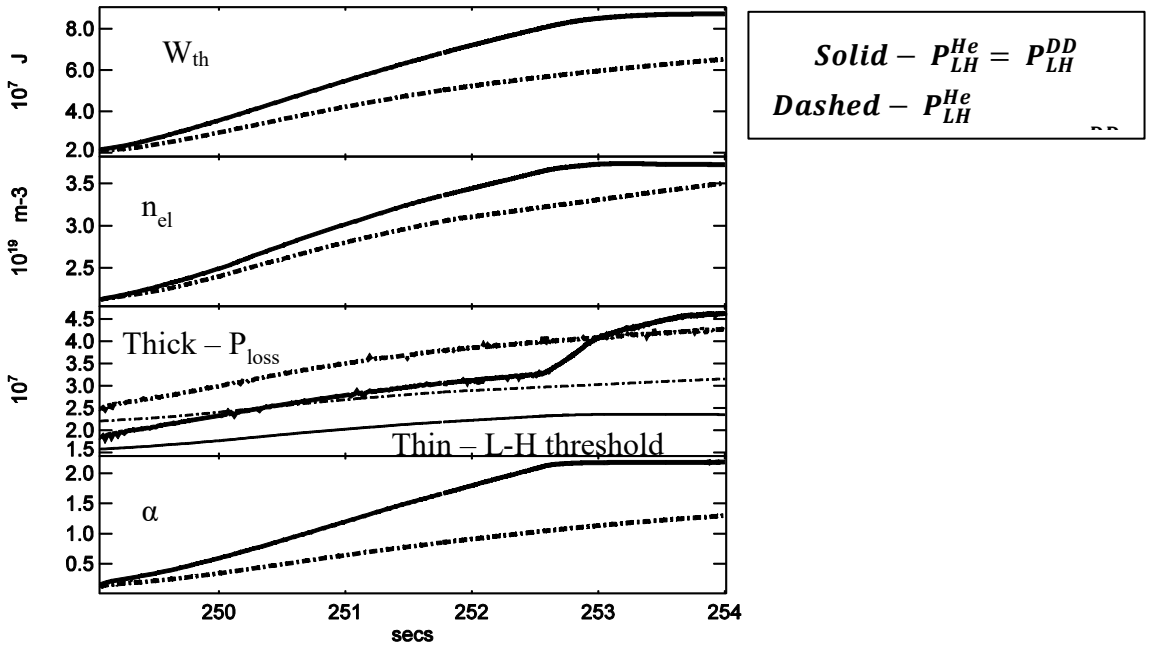

Figure 6. H-mode access for 7.5MA/2.65T He ITER plasma with 33MW NB and 20MW ECRH. With an optimistic assumption for the L-H power threshold (solid assuming same threshold for D and He plasmas) the He plasma reaches the ELMy H-mode (ballooning parameter $\alpha=\alpha_{crit}=2.1$) in ~3.5s after the NB has been turned on. As we have applied the continuous ELM model in JINTRAC, the pedestal pressure gets clamped at $\alpha=\alpha_{crit}$ and the thermal energy content (W_{th}) and line-average density (n_{el}) saturate. The case with a realistic L-H threshold (chain, He H-mode threshold 1.4 times that of D plasmas) the plasma enters the H-mode but is still far from stationary ELMy H-mode conditions ($\alpha\approx1.4$) at the end of the simulation time.

After 10s of the current-ramp simulation, the density and the on-axis electron and ion temperatures have almost reached the target values that are modelled for steady-state L-mode plasmas at 7.5MA/2.65T (Figure 4.). Because the plasma current had reached only 5.5MA the simulation should be continued at a constant density with varying current to achieve the flat top plasma current value of 7.5 MA. However, at this core plasma density, current and ECRH power the inner divertor was close to detachment, and we could not complete with increasing current due to numerical instabilities. Indeed, the steady-state He L-mode simulations at 7.5MA/2.65T with 20 MW of ECRH could only reach line-average densities of ~$2.1\text{x}10^{19}\text{m}^{-3}$ with a He gas fuelling rate of $7.0\text{x}10^{21}$/s before the He radiation front in the divertor started to move to the X-point and render the divertor conditions unstable. This density is lower than the target feedback value for the current ramp at 7.5 MA, 50% of the Greenwald limit corresponds to ~ $3.0\text{x}10^{19}\text{m}^{-3}$), which is similar to the required value for unrestricted NBI operation (at full power of 33 MW) in He plasmas, which is required for H-mode access in these plasma conditions. In order to determine if shine-through losses would be a problem in the access phase, we have performed a simulation in which full NBI power is injected in a 7.5 MA/2.65T He plasma with 20 MW of ECRH heating and line-average density of ~$2.1\text{x}10^{19}\text{m}^{-3}$ and modelled the density rise after the H-mode transition. The NBI deposition and shine-through losses have been evaluated with ASCOT and, as shown in Figure 5, it is found that the plasma density increases rather quickly after the H-mode transition so that shine-through losses reduce from 20% to 3-6 % in about 5 s so that the resulting power fluxes on the first wall are expected to remain acceptable in this phase [8].

To test the sensitivity of H-mode access in He to threshold assumptions we have performed simulations for two levels of L-H transition in He, one is optimistic assuming the same threshold for He and D plasmas as seen in ASDEX-Upgrade, and the other one more realistic, assuming that the He H-mode threshold is higher than that of D by a factor 1.4 as experimentally observed in JET, DIII-D, Alcator C-Mod, etc.. As expected, the lower L-H threshold in the optimistic case allows for a faster transition into ELMy H-mode (Figure 6) with the edge stability ballooning parameter reaching $\alpha=\alpha_{crit}=2.1$ in ~3.5s after the NB has been turned on. On the other hand, after 5s the case with the a less optimistic threshold is still well within the ELM-free phase of the transition ($\alpha\approx1.4<\alpha_{crit}=2.1$). In this case a faster access to ELMy H-mode would require the use of the available 20 MW ICRH besides the 33 MW of NB used in these simulations.

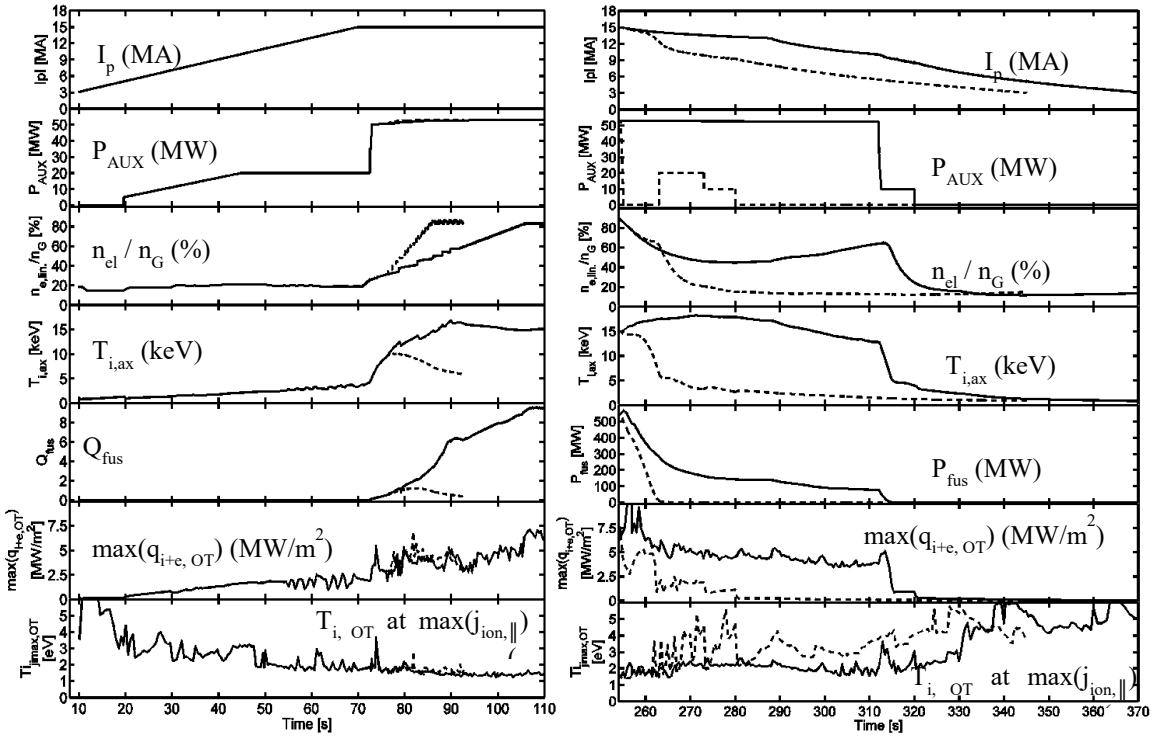

Figure 7. JINTRAC modelling results of the current-ramp up and access to Q = 10 (left) for the DT ITER baseline scenario with L-H transition at 15MA with 33MW NB +20MW ECRH. Slow (solid) and fast (dashed) density ramp after the transition show that a too fast density ramp-up prevents access to Q = 10 conditions. Current ramp-down and exit from Q =10 conditions (right) in the ITER DT baseline scenario with the H-L transition by switching of the additional heating at 15MA (dashed) and at ~10MA (solid).

4. JINTRAC simulations of the ITER 15 MA/5.3 T Q = 10 baseline plasma scenario

Full simulations of the Q = 10 baseline scenario from X-point formation in the current ramp-up to X-point to limiter transition in the current ramp-down have been performed. The current ramp-up and ramp-down phases are important for the achievement of ITER fusion production goals. During the current ramp-up the plasma current is increased towards the target values for the high Q burning plasma phase. In the ramp-down phase the plasma must exit the burning conditions and need to be terminated in a controlled way while avoiding disruptions both in cases in which the termination can be performed over long timescales and when the timescales are shorter following, for instance, malfunctions of one or more ancillary systems (e.g. heating and current drive systems).

Our simulations of the baseline scenarios have been performed from early X-point formation at 3MA/5.3T at 10s, which allows the use of auxiliary heating to reduce the flux consumption in the ramp-up phase. The simulated current ramp-up rate of 200kA/s leads to 15MA being reached at 70s (Figure 7, left), which is well within the capabilities of the ITER poloidal field system. At this stage the additional heating is increased to trigger the H-mode transition which finally results in the stationary 15MA/5.3T ELMy H-mode plasma condition with a Greenwald density fraction of 85%, and a fusion gain of Q=10. Our simulations have demonstrated that such plasma scenario is indeed feasible within the physics basis and models included in the JINTRAC modelling code (which has been compared to experiment) and without exceeding physics or design limits of the ITER components (e.g. divertor power fluxes). This has been demonstrated for both stationary conditions corresponding to specific instants of the Q =10 scenario as well as for the scenario as a whole, as illustrated in (Figure 7).

The studies of the achievable density in ITER DT L-modes show that for a given input power, the core density increases with the gas rate and then saturates[5][6][38], following the same qualitative trends as for H and He plasmas in Section 3. If the gas rate is further increased, the divertor plasma enters a deep detached state that leads to the thermal instability of the solution and the termination of the simulation. Our JINTRAC simulations indicate that in the current ramp-up of the Q =10 a Greenwald density fraction of less than 35% can be expected with gas fuelling only for 20MW of RF heating[6][38]. Although higher fractions with more radio frequency (RF) heating can be achieved with gas fuelling only, especially at lower currents, it is more effective to use pellet fuelling if higher densities are required during the ramp-up, in qualitative agreement with the H L-mode simulations in Section 3. It is important to note, however, that during the DT phase the ITER NBI will be operated in D at 1 MeV (for the full power of 33 MW) and that the density required for unrestricted NBI operation in DT plasmas (~2.2 $10^{19}m^{-3}$) is much lower than for He and H so that for ~ 0.35 n_{GW} unrestricted NBI operation is possible for currents above 8 MA. At present NB injection at such low levels of plasma currents is not considered in the Q = 10 scenario but if they were required, this would be possible by dominant pellet fuelling as demonstrated in Section 3.

Aligned with previous JINTRAC core-only predictions[13], our fully integrated core+SOL/divertor modelling simulations indicate that the build-up of the fusion power, and corresponding α heating, is essential (besides additional heating) to the access to stationary ELMy H-mode burning plasma conditions [38] in order to provide sufficient margin above the L-H threshold power. This requires a careful optimization of the plasma fuelling in the H-mode access phase so that the core ion temperature can increase to values in which DT fusion reaction rates are significant and can contribute to the total heating power and the further improvement of the H-mode performance through the concomitant reduction of the transport in the ETB. This is illustrated in Figure 7 (left) where two pellet fuelling rates are applied after the L-H transition in the ITER Q = 10 scenario. For the highest rate the plasma returns to L-mode after a brief ELM-free phase following the H-mode transition because of the insufficient α heating and edge power flow. In this Q = 10 scenario the divertor power loads remains under the 10 MWm^{-2} limit without the need for extrinsic impurity seeding (Ne) in the ELM-free phase up to Q ~ 5. For higher Q phases and the stationary conditions Ne seeding is required to maintain the divertor power flux under the limit above. Undeniably, the need to maintain sufficient divertor radiation to lower the divertor flux to acceptable values introduces specific complications when considered together with core plasma fuelling with pellets and the associated particle flux transients. Our simulations of pellet fuelling of 15MA/5.3T ITER ELMy H-mode Q = 10 plasmas with acceptable divertor power fluxes, which requires a separatrix density ~$5.5x10^{19}m^{-3}$ and Ne seeding, show that the pellet size needs to be carefully optimised to achieve a fully integrated scenario (including fuelling, particle and power exhaust); pellets with a particle

content larger than $5.5x10^{21}$ atoms lead to deep transient divertor detachment after pellet injection and the thermal collapse of the plasma solution [38].

The current ramp-down is typically expected to be twice as long as the ramp-up phase. At the beginning or during the current ramp-down phase the plasma exits the burning conditions and during the ramp-down itself the plasma current is reduced to ensure a controlled termination avoiding vertical stabilities and disruptions [39]. This is a complex phase as the control of vertical stability is linked to plasma shape and radial plasma position control so that fast losses of plasma energy (such as during H-L transitions) can lead both to large divertor power fluxes and to radial inwards shifts of the plasma and loss of vertical stability if the limits of the vertical stabilisation systems in ITER are exceeded in this phase.

To study plasma behaviour in the ramp-down phase we have considered a current ramp-down evolution from 15MA/5.3T Q=10 burning plasma to 3MA/5.3T in ~ 90-120s depending on the plasma current at which the H-L transition takes place (Figure 7, right). Our model of the ETB transport modification with margin above the H-mode threshold (Eq. 6) results in a phase of ~ 5s for the plasma energy to decrease from H-mode values to L-mode values in this exit phase. This timescale agrees with present experiments [13][40] and allows the sustainment of good radial position control in this phase. On the other hand, power fluxes to the divertor can be very substantial in the initial phase of the H-mode termination. To avoid the divertor power fluxes to exceed the limit of 10 MW m^{-2} and W sputtering to significantly increased (W is not modelled in our simulations but a guideline of ~5 eV at the location of maximum ion flux is taken for significant W sputtering to take place), it is necessary to use Ne seeding. In later phases where the edge power flow decrease (due to the reduction of dW/dt as plasma energy decreases), Ne seeding must be carefully tuned down or even turned-off to ensure that the Ne level in the plasma is reduced by the pumping system to avoid deep detachment of the divertor in the lower power phases of the ramp-down. In our modelling the tuning of plasma fuelling, Ne seeding, etc., has been done by manual adjustment with the results illustrated in Figure 7 (right) for two examples: a complete switch-off of the additional heating at the end of the 15 MA flat top; and for an H-L transition in the current ramp-down itself (at around 10 MA). While these simulations show that integrated scenarios for burn termination ensuring stable plasma behaviour and acceptable divertor power fluxes can be obtained with the ITER Heating & Current Drive and fuelling/impurity seeding systems, to progress further in the optimization of this complex phase requires the development of more sophisticated feedback loops in the JINTRAC modelling suite that avoids the computationally intensive trial and error approach that been followed to achieve the results in Figure 7.

5. Summary and Conclusions

In this paper, we have presented integrated core-SOL/divertor transport simulations with JINTRAC of the non-active and nuclear phases of ITER plasmas scenarios, including the first core-SOL/divertor simulations of He plasmas and of the full DT Q = 10 scenario including the current ramp-up/down diverted phases. We have shown that pellet injection is the most effective way to increase plasma density in L-mode plasmas and that it will be required to provide unrestricted NB operation in hydrogen H-mode plasmas. For He plasmas gas fuelling alone is sufficient to provide this operation by access to H-mode conditions at 7.5 MA/2.65T that reduces the shine-through losses by the associated density increase but the operational range in these conditions is not wide. For DT plasmas the use of pellet fuelling is less essential for unrestricted NBI operation due to the lower shine-through losses in these conditions. These results show that commissioning and operation of the ITER NB system to full power should be possible in 15 MA/5.3T L-mode hydrogen plasmas, in conjunction with at 20MW of ECRH, using pellet fuelling. Similarly, He H-mode plasmas at 7.5MA/2.65 T with an additional heating

level of 53-73 MW can be achieved, which allows the characterisation of H-mode plasmas and the demonstration of ELM control schemes to take place in the non-active phase before ITER DT operation.

Our integrated simulations show that access to high Q conditions in ITER DT plasmas requires an optimized build-up of the α heating after the L-H transition because the margin above the L-H threshold provided by the additional heating in ITER is moderate for high current 5.3T DT plasmas in ITER. This α heating optimized build-up can be achieved by tuning of the density rise through pellet fuelling with an initial low fuelling rate phase to allow the ion temperature to build up in the plasma to, typically Q ~5, followed by a larger rate to provide the density rise to the stationary Q = 10 ELMy H-mode conditions with 85% of n_{GW}. For the high Q transient and stationary phases of the Q =10 scenario (typically Q > 5) Ne seeding is required to maintain the divertor power fluxes under the 10 MWm^{-2} limit. This introduces a complex interaction between power flux control, particle control and fuelling when pellets are used to fuel the plasma due to the intrinsic particle fluxes that they cause. Pellets beyond a given size can trigger transient deep divertor detachment leading to the thermal collapse of the solution. Therefore, when considering fuelling optimization of ITER high Q plasmas it is essential to consider these other aspects through adequate integrated modelling to obtain a fully integrated simulation of the scenario; individual optimization of separate aspects of particle and power control of the ITER high Q scenarios may be misleading. Our integrated JINTRAC simulations of the exit from burn in the Q = 10 scenario show that the flexibility of the ITER systems can provide conditions in which plasma position control can be maintained and power fluxes to the divertor remain under the acceptable limit. This requires careful optimization of fuelling and impurity (Ne) seeding to ensure it provides the required divertor radiation in the phases with high edge power flow (initial phase of the H-mode termination) and that this is sufficiently low in later phases of the termination when edge power fluxes are lower (end of H-mode and L-mode phases).

While these initial simulations show that the flexibility of the ITER fuelling, heating and impurity seeding systems is appropriate to ensure a robust access to/exit from and sustainment of Q = 10 burning plasmas, a detailed optimisation of their application for a wide range of ITER high Q scenarios requires new feedback loops to be implemented in JINTRAC and this is the focus of on-going work.

APPENDIX 1: Assumptions on energy recycling in the SOL/divertor and their impact on simulation results

A1.1 Introduction

In this appendix, we explore how different modelling assumptions, with regards to the energy of the recycling neutrals in the SOL/divertor, affect the properties of the overall plasma simulations and, in particular the divertor plasma. JINTRAC has historically assumed that the plasma ion energy source from charge exchange always acts as a sink (i.e. charge exchange from reflected neutrals always cools the ions), because the wall fast reflection of energetic neutrals is considered to be negligible. This assumption is reasonable when the plasma facing components (PFCs) are made from low Z materials (like C or Be), but increased reflection of fast neutrals arises in the case of PFCs made from higher Z materials (like W). Reflection of energetic neutrals increases the plasma ion energy source, and charge exchange can become a source of ion heating in the SOL/divertor. All the ITER simulations in the main part of this paper were carried out using the original JINTRAC assumption that reflected neutrals only cool the plasma. In this Appendix we repeat a few reference ITER simulations from the main paper,

using an improved model in JINTRAC to allow for a positive heat source from reflected energetic neutrals. This demonstrates that the improved model has only a modest impact on the predicted ITER scenarios; to assess worst possible cases we consider conditions with high ion divertor temperatures where the effect under study should be largest although these are not realistic for ITER operation with a W divertor because of excessive W sputtering due to high ion temperatures and divertor power fluxes exceeding 10 MWm^{-2} in some cases.

When an ion hits a PFC one of three processes can happen, 1) the particle and its energy are absorbed by the wall; 2) thermal reflection, i.e. the ion returns as a molecule with PFC temperature and a cosine angular distribution; or 3) fast reflection, i.e. the ion returns as an atom with a fraction of the impact energy and angular distribution calculated by the TRIM database[41][42]. For absorption and thermal reflections all or most of the energy is absorbed by the wall material and it would be correct to assume that the thermally reflected molecules are colder than the plasma and that the ensuing charge exchange process would cool the ions. Moreover, these two processes are the most likely ones in absorbing materials with an atomic mass close the plasma fuel species, such as Carbon. In Beryllium, a material with much lower fuel retention than Carbon [43][44] but also lower mass, thermal reflections dominate as well. The fuel retention in Tungsten is also very low, but the much higher atomic mass promotes fast reflections where, on average, ~50% of the impact energy [41][42] returns to the plasma via highly energetic atoms. These may heat the ions through charge exchange processes and thus keep the divertor plasma hotter and reduce the likelihood of full detachment.

A1.2 L-mode comparisons for ITER H plasmas

In this case we study the effect of the different modelling assumption of energy recycling as described in A1.1 on a pellet-fuelled 10MA/5.3T pure Hydrogen plasma with 20MW of ECRH. To ensure acceptable divertor power fluxes, gas is fuelled at a rate of $5.0x10^{20}s^{-1}$ besides the fuelling by pellets ($90mm^3/5.3x10^{21}$ particles), which we inject at a frequency of 4Hz.

Figure. A. 1 shows that the volume-averaged core ion density and on-axis ion temperature are not affected by the divertor energy recycling assumptions but that there is a very minor effect on the outer-mid-plane (OMP) electron and ion densities and temperatures. This is supported by the nearly identical OMP profiles at the end of the simulation (Figure. A. 2). Only at the divertor plates can we observe the impact of the different energy recycling assumptions. At the outer divertor (Figure. A. 3) the densities and temperatures are somewhat higher for the correct W energy recycling assumptions, whereas at the inner divertor (Figure A. 4) we only see an increase in the target plasma temperatures. We have also obtained very similar results for pellet-fuelled ($90mm^3/5.3x10^{21}$ particles, injection frequency 3.3-4Hz) 15MA/5.3T pure Hydrogen plasma simulations with 20MW of ECRH and with a gas rate of $5.0x10^{20}s^{-1}$. The main differences between the 10 and 15 MA cases are: 1) a slight increase of a few eV in the OMP ion temperature close to the plasma boundary for 15 MA, 2) a ~$0.1x10^{19}m^{-3}$ increase of both ion and electron OMP separatrix densities for 15 MA, and 3) possibly a more pronounced increase in the inner target temperatures at 15 MA.

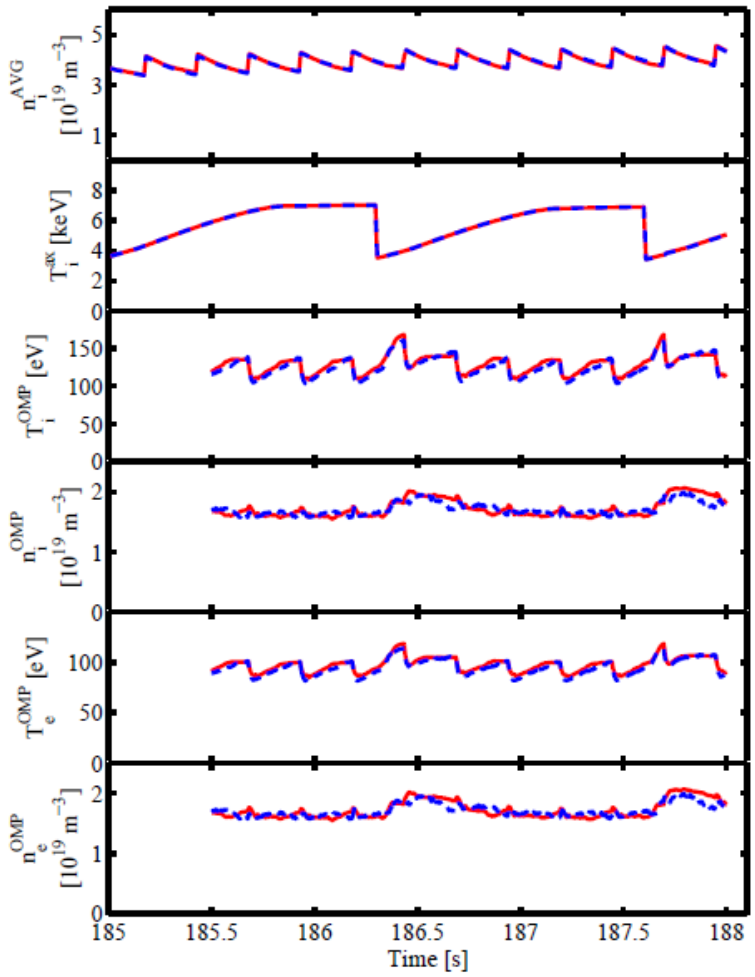

Figure. A. 1: Comparison of time traces with W (red, solid) and C (blue, dashed) divertor energy assumptions for a 10MA/5.3T ITER Hydrogen L-mode with 20MW ECRH and no impurities. The applied gas rate was 5.0x1020s^{-1} and pellets (90mm3/5.3x10^{21}particles) were injected with a frequency of 4Hz. Sawtooth crashes are visible in the on-axis ion temperature time trace.

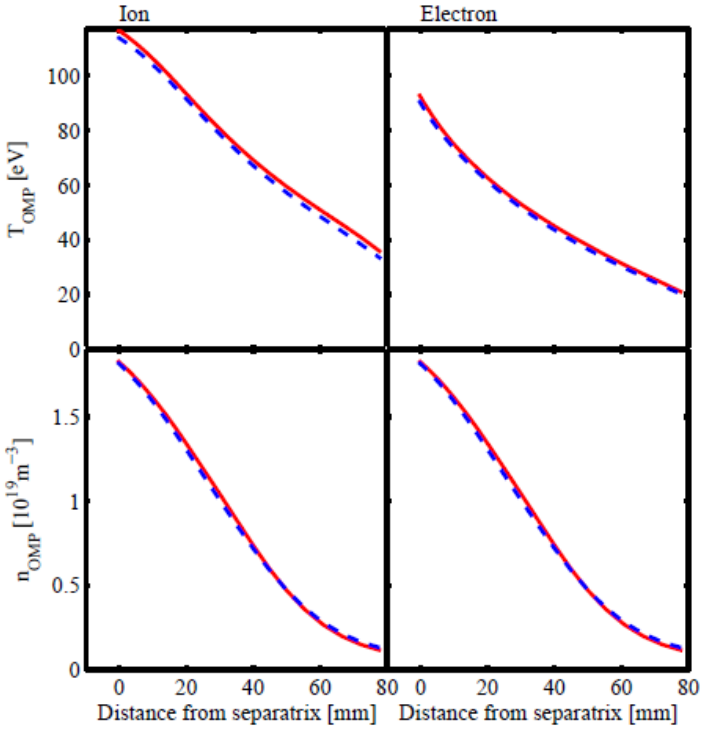

Figure. A. 2: Comparison of the outer-mid-plane SOL profiles at 188s of ion (left) and electron (right) temperatures (top) and densities (bottom) with W (red, solid) and C (blue, dashed) divertor energy recycling assumptions for a 10MA/5.3T ITER Hydrogen L-mode with 20MW ECRH and no impurities. The applied gas rate was $5.0x10^{20}s^{-1}$ and pellets ($90mm^3/5.3x10^{21}$particles) were injected with a frequency of 4Hz.

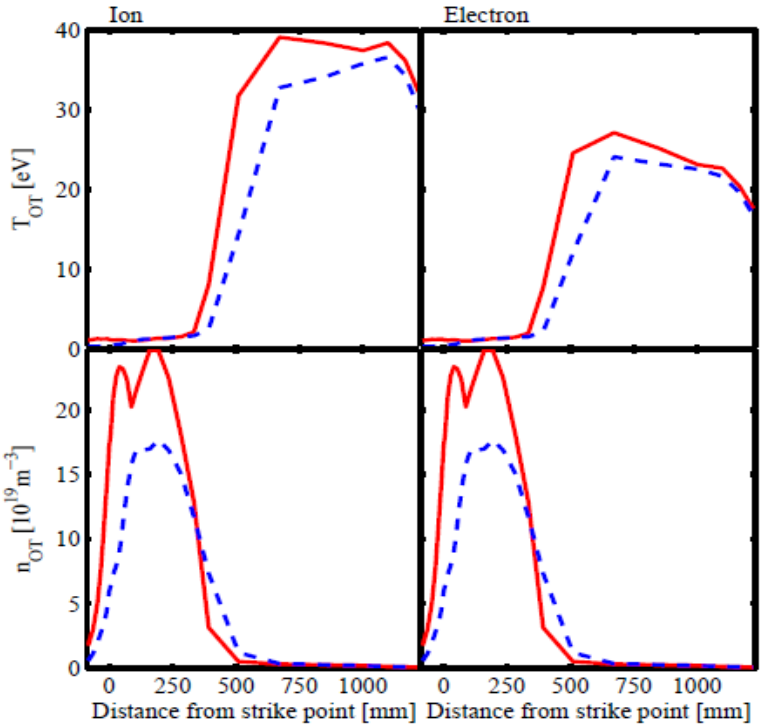

Figure. A. 3: Comparison of outer target profiles at 188s of ion (left) and electron (right) temperatures (top) and densities (bottom) with W (red, solid) and C (blue, dashed) divertor energy recycling assumptions for a 10MA/5.3T ITER Hydrogen L-mode with 20MW ECRH and no impurities.

The applied gas rate was 5.0x1020s^{-1} and pellets (90mm^3/5.3x10^{21}particles) were injected with a frequency of 4Hz.

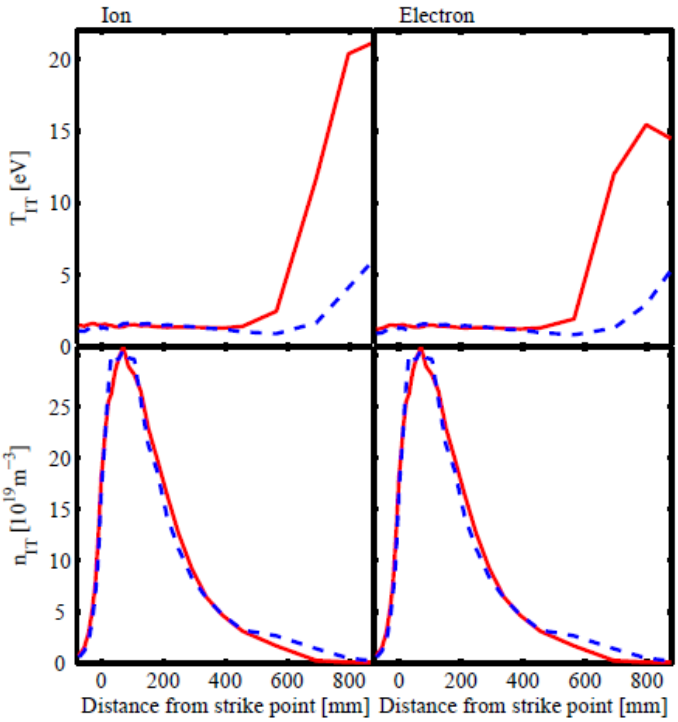

Figure A. 4: Comparison of inner target profiles at 188s of ion (left) and electron (right) temperatures (top) and densities (bottom) with W (red, solid) and C (blue, dashed) divertor energy recycling assumptions for a 10MA/5.3T ITER Hydrogen L-mode with 20MW ECRH and no impurities. The applied gas rate was 5.0x1020s^{-1} and pellets (90mm^3/5.3x10^{21}particles) were injected with a frequency of 4Hz.

A1.3 H-mode comparisons for ITER DT plasmas

In this section, we examine the impact of the energy-recycling modelling assumptions on a 15MA/5.3T DT H-mode with 33MW of NB and 20MW of ECRH heating. On top of a gas rate of 1.0x10^{20}s^{-1} we simulate pellet fuelling (50/50 DT, 74mm^3/4.6x10^{21}particles) to achieve a target density of ~ 1.0 x10^{20}m^{-3}, as required for Q =10 operation in ITER. JINTRAC automatically adjusted the frequency of the pellets to reach and maintain this target through appropriate feedback. These simulations also included impurities, Be sputtered from the main vessel wall and Ne from seeding (1.0x10^{20}s^{-1}) to reduce the divertor power fluxes although the maximum power flux fluctuated between 5-30 MWm^{-2} at the outer target and between 5-15 MWm^{-2} at the inner target. Even if this case uses the latest assumptions for the ion energy source model, it should be noted that these power loads are overestimates as they have not been corrected for the neutral reflected energy.

For the two different energy-recycling assumptions, the core time traces of the ion volume-average density and on-axis temperature are quite similar (Figure A. 5). This holds true for the time traces of the OMP separatrix temperatures as well. However, the OMP separatrix density with W energy recycling assumptions evolves with time whereas it remains rather stationary with C energy recycling assumptions. This is likely due to a slight difference in the particle flux crossing the separatrix from the core into the SOL due to the higher energy of the recycled neutrals and increased core ionisation, which allows for a build-up of the OMP density in the W energy recycling assumptions case. This is also the cause of the different timings of the pellet injections as a pellet is not triggered unless the density goes below its target value by the

feedback loop. Besides these small differences, the OMP SOL profiles are nearly identical (Figure A. 6). There are small variations (≤10% at peak values) in the OT divertor profiles (Figure A. 7), while we can observe a more significant difference in the IT divertor ion temperature (~30% at peak value) even if the other IT profiles differ by about 10% at peak values (Figure A. 8) It is important to remember that the plasmas modelled correspond to well attached conditions with minimal ionisation and recombination sources at the strike points (not shown) as these are expected to show the largest differences due to two energy recycling assumptions.

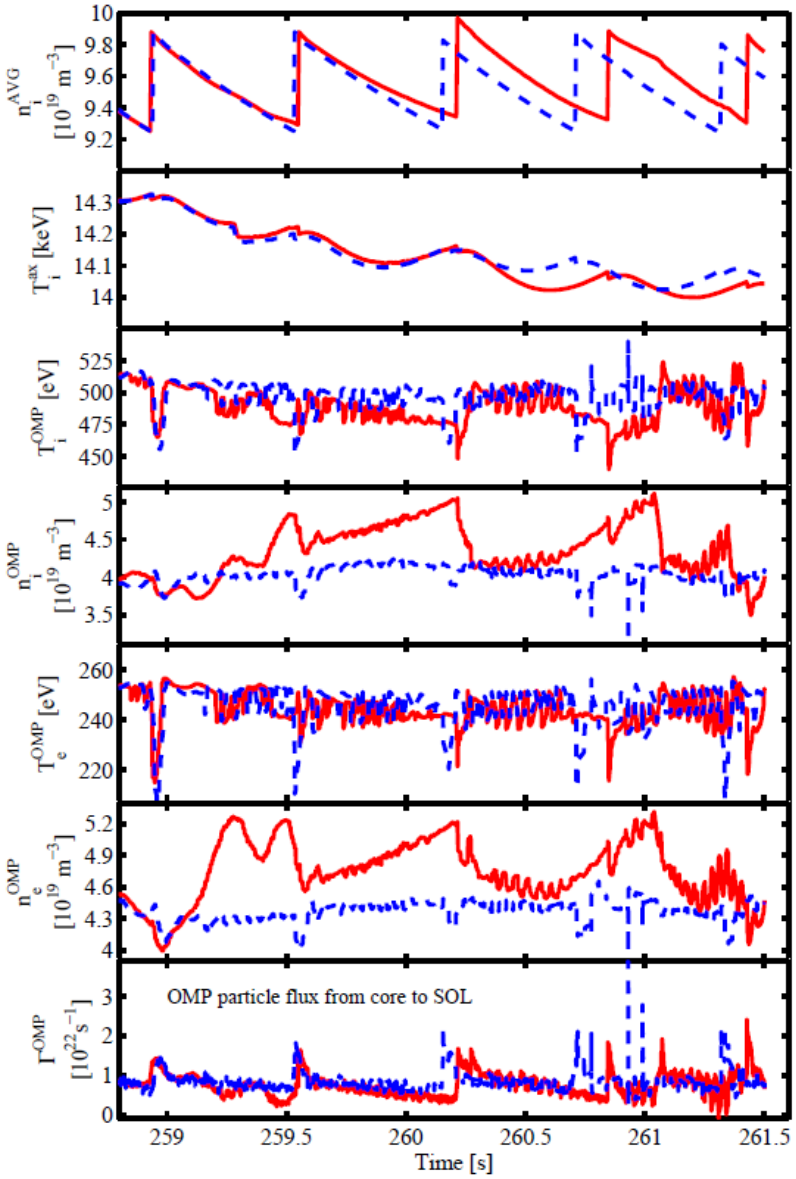

Figure. A. 5: Comparison of time traces with W (red, solid) and C (blue, dashed) divertor energy recycling assumptions for a 15MA/5.3T ITER DT H-mode with 53MW auxiliary heating and including intrinsic and extrinsic impurities, Be and Ne, respectively. The applied gas rate was $1.0x10^{22}s^{-1}$ and pellets (50/50 DT, $72mm^3/4.2x10^{21}$ particles) were injected with an automatically adjusted frequency to achieve a line-average density of ~$1.0x10^{20}m^{-3}$.

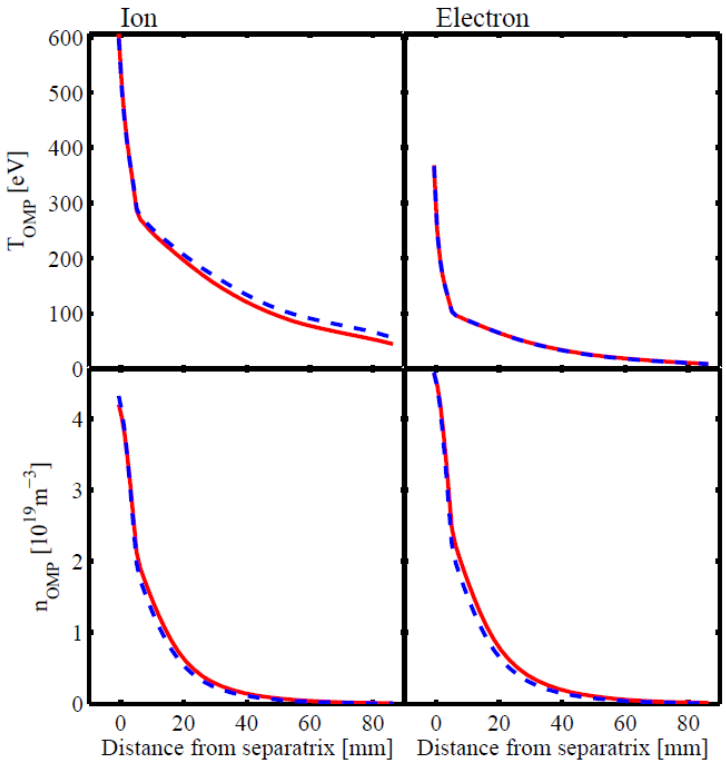

Figure. A. 6: Comparison of outer-mid-plane SOL profiles at 261.5s of ion (left) and electron (right) temperatures (top) and densities (bottom) with W (red, solid) and C (blue, dashed) divertor energy recycling assumptions for a 15MA/5.3T ITER DT H-mode with 53MW auxiliary heating and including intrinsic and extrinsic impurities, Be and Ne, respectively. The applied gas rate was $1.0x10^{22}s^{-1}$ and pellets (50/50 DT, $72mm^3/4.2x10^{21}$ particles) were injected with an automatically adjusted frequency to achieve a line-average density of ~$1.0x10^{20}m^{-3}$.

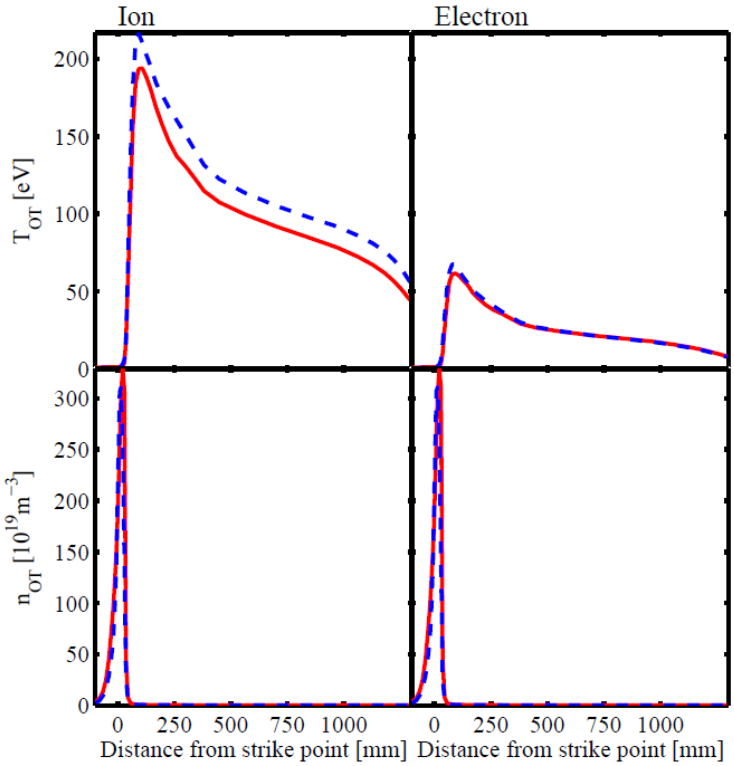

Figure A. 7: Comparison of outer target profiles at 261.5s of ion (left) and electron (right) temperatures (top) and densities (bottom) with W (red, solid) and C (blue, dashed) divertor energy

recycling assumptions for a 15MA/5.3T ITER DT H-mode with 53MW auxiliary heating and including intrinsic and extrinsic impurities, Be and Ne, respectively. The applied gas rate was $1.0x10^{22}s^{-1}$ and pellets (50/50 DT, $72mm^3/4.2x10^{21}$ particles) were injected with an automatically adjusted frequency to achieve a line-average density of ~$1.0x10^{20}m^{-3}$.

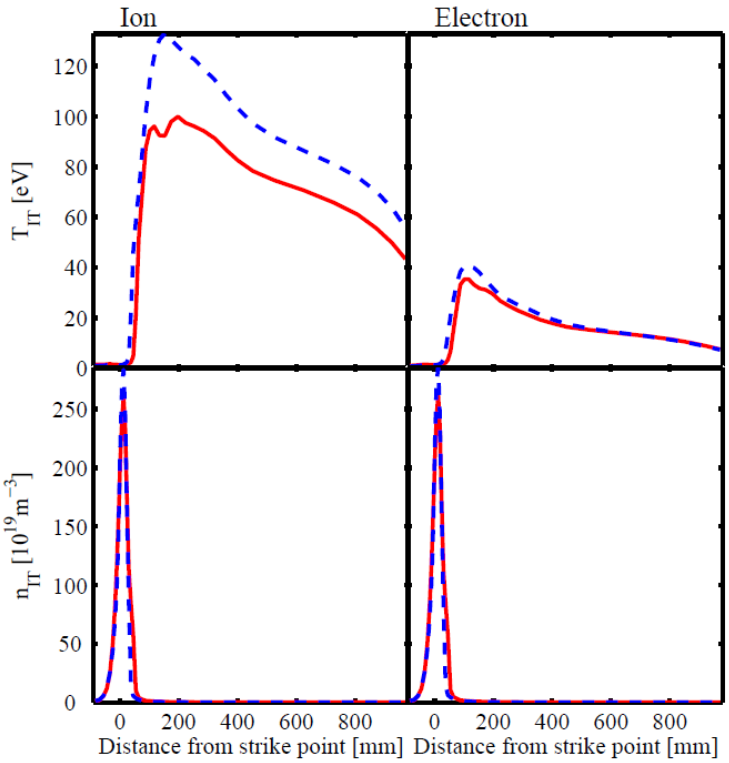

Figure A. 8: Comparison of inner target profiles at 261.5s of ion (left) and electron (right) temperatures (top) and densities (bottom) with W (red, solid) and C (blue, dashed) divertor energy assumptions for a 15MA/5.3T ITER DT H-mode with 53MW auxiliary heating and including intrinsic and extrinsic impurities, Be and Ne, respectively. The applied gas rate was $1.0x10^{22}s^{-1}$ and pellets (50/50 DT, $72mm^3/4.2x10^{21}$ particles) were injected with an automatically adjusted frequency to achieve a line-average density of ~$1.0x10^{20}m^{-3}$.

A1.4 Conclusions

For ITER hydrogen and DT plasmas cases with a W divertor and Be main chamber wall, we have investigated the consequences of different assumptions on ion-energy recycling at the divertor and their effects on the SOL and divertor plasmas, through their impact on charge-exchange energy balance, and on the global plasma behaviour in general and divertor conditions in particular. As our simulations show for ITER plasmas, where ionization lengths of recycling neutrals are much smaller than plasma dimensions, there is a negligible impact on the core plasma parameters and a minor impact on the SOL and divertor parameters. The minor effects associated with higher energy of the recycled ions on the W divertor target leads to slightly increased divertor temperatures, thus requiring a higher separatrix density or impurity seeding level to achieve the conditions required for divertor detachment. On this basis we can conclude that the evaluation of the density range achievable with gas fuelling in ITER provided by our studies in the main part of this paper is a conservative lower estimate; inclusion of the proper energy recycling assumptions for the ITER divertor is likely to increase this range although, from the studies in this appendix, this increase will be small.

References

[1] The ITER Research Plan, ITER Technical Report ITR-18-03, ITER Organization 2018.

[2] KÖCHL, F., et al., "Modelling of transitions between L- and H-mode in JET high plasma current plasmas and application to ITER scenarios including tungsten behaviour", Nuclear Fusion **57**, 086023 (2017)

[3] KUKUSHKIN, A.S., et al., "Basic divertor operation in ITER-FEAT", Nuclear Fusion, **42**, 187 (2002)

[4] KUKUSHKIN, A.S., et al., "Physics requirements on fuel throughput in ITER", Journal of Nuclear Materials, **415**, 497 (2011)

[5] ROMANELLI, M., et al., "Modelling of plasma performance and transient density behaviour in the H-mode access for ITER gas fuelled scenarios", Nuclear Fusion, **55**, 093008 (2015)

[6] DA SILVA ARRESTA BELO, P., et al., "Modelling of plasma performance and transient density behaviour in the H-mode access for ITER gas fuelled scenarios", Europhysics Conference Abstracts, 39, EPS 2015, P4.120

[7] POLEVOI, A.R., et al., "Analysis of fuelling requirements in ITER H-modes with SOLPS-EPED1 derived scalings", Nuclear Fusion **57**, 022014 (2017)

[8] SINGH, M.J., et al., "Heating neutral beams for ITER: negative ion sources to tune fusion plasmas", New Journal Physics, **19**, 055004 (2017)

[9] RIGHI, E., et al., "Isotope scaling of the H mode power threshold on JET", Nuclear Fusion, **39**, 309 (1999)

[10] RYTER, F., et al., "H-mode threshold and confinement in helium and deuterium in ASDEX Upgrade", Nuclear Fusion. 49, 062003 (2009).

[11] GOHIL, P., et al., "L-H Transition studies on DIII-D to determine H-mode access for operational Scenarios in ITER", Nuclear Fusion, 51, 103020 (2011).

[12] MCDONALD, D.C., et al., "JET helium-4 ELMy H-mode studies," EFDA-JET report No. EFDA–JET–CP(10)08/24 (2011).

[13] LOARTE, A., et al., "Plasma density and temperature evolution following the H-mode transition at JET and implications for ITER", Nuclear Fusion, 53, 083031(2013)

[14] GARZOTTI, L., et al., "Integrated core-SOL modelling of fuelling, density control and divertor heat loads for the flat-top phase of the ITER H-mode D-T scenario", to be submitted to Nuclear Fusion.

[15] ROMANELLI, M., et al., "JINTRAC: A System of Codes for Integrated Simulation of Tokamak Scenarios", Plasma and Fusion Research, 9, 3403023 (2014)

[16] CENACCHI, G. and TARONI, A., "A free-boundary plasma transport code", JET-IR(88)03, 1988

[17] LAURO-TARONI, L., et al., "Impurity Transport of High Performance Discharges in JET", 1994 Proc. 21st EPS Conf. on Controlled Fusion Plasma Physics (Montpellier, France, 27 June–1 July 1994) vol 18B p 102 (1994)

[18] SIMONINI, R., et al., "Models and Numerics in the Multi-Fluid 2-D Edge Plasma Code EDGE2D/U", Contrib. Plasma Phys., 34, 368 (1994)

[19] REITER, D., "Progress in two-dimensional plasma edge modelling", J. Nucl. Mater., 196-198, 80-89 (1992)

[20] KOTOV, V., et al., “Verification of the 2D Tokamak Edge Modelling Codes for Conditions of Detached Divertor Plasma”,Contrib. Plasma Phys., 50, 292–298 (2010)

[21] HARTING, D., et al., “D-T segregation study for JET L- and H-mode plasmas by fully core-edge coupled simulations with JINTRAC”, PSI Rome (2016)

[22] KUKUSHKIN, A.S., et al., “Impact of potential narrow SOL heat flux on H-mode access in ITER”, Nuclear Fusion, 53, 123024 (2013)

[23] KUKUSHKIN, A.S., et al., “ITER divertor performance in the low-activation phase”, Nuclear Fusion, 53, 123025 (2013)

[24] LOARTE, A., et al, “”, Journal of Nuclear Materials 463, 401–405 (2015)

[25] GARZOTTI, L., et al., “Neutral gas and plasma shielding scaling law for pellet ablation in Maxwellian plasmas. Nucl. Fusion”, 37, 1167 (1997)

[26] PEGOURIE, B., et al., “Homogenization of the pellet ablated material in tokamaks taking into account the ∇B-induced drift”, Nuclear Fusion, 47, 44 (2007)

[27] WALTZ, R.E., et al., “A gyro-Landau-fluid transport model”, Phys. Plasmas 4 2482 (1997)

[28] HOULBERG, W.A., et al., “Bootstrap current and neoclassical transport in tokamaks of arbitrary collisionality and aspect ratio”, Phys. Plasmas, 4, 3230 (1997)

[29] CHALLIS, C.D., et al., “Non-inductively driven currents in JET”, Nuclear Fusion 29, 563 (1989).

[30] HIRVIJOKI, E., et al., “ASCOT: Solving the kinetic equation of minority particle species in tokamak plasmas”, Computer Physics Communications, 185, 1310-1321, (2014)

[31] ERIKSSON, L.-G. and HELLSTEN, T., “A model for calculating ICRH power deposition and velocity distribution”, Physica Scripta, 52, 70 (1995)

[32] FARINA, D., “GRAY: a quasi-optical ray tracing code for electron cyclotron absorption and current drive in tokamaks”, IFP-CNR Internal Report, FP 05/1 (2005)

[33] MARTIN, Y. R., et al., “Power requirement for accessing the H-mode in ITER”, Journal of Physics: Conference Series, 123, 012033 (2008)

[34] SNYDER, P.B., et al., “A first-principles predictive model of the pedestal height and width: development, testing and ITER optimization with the EPED model”, Nuclear Fusion ,51, 103016 (2011)

[35] PARAIL, V., et al., “Self-consistent simulation of plasma scenarios for ITER using a combination of 1.5D transport codes and free-boundary equilibrium codes”, Nuclear Fusion, 53, 113002 (2013)

[36] LOARTE, A., et al., “Progress on the application of ELM control schemes to ITER scenarios from the non-active phase to DT operation”, Nuclear Fusion, **54**, 033007 (2014)

[37] KADOMTSEV, B.B., “Disruptive instability in Tokamaks”, Sov. J. Plasma Phys., 1, No. 5 Sept. Oct., p. 389 (1975)

[38] GARZOTTI, L., et al., “Integrated modelling of fuelling and density control in ITER”, Europhysics Conference Abstracts, 40, EPS 2016, O4.113

[39] SIPS, A.C.C., et al., “Progress in preparing scenarios for operation of the International Thermonuclear Experimental Reactor”, Physics of Plasmas, 22, 021804 (2015)

[40] DE VRIES, P.C., et al., “Multi-machine analysis of termination scenarios with comparison to simulations of controlled shutdown of ITER discharges”, Nucl. Fusion, **58**, 026019 (2018)

[41] ECKSTEIN, W. and HEIFETZ, D.B., “Data sets for hydrogen reflection and their use in neutral transport calculations”. MPI-Garching Report IPP 9/59, MPI-Garching, August 1986., J.Nucl.Mater. 145-147, p332 (1987)

[42] BATEMAN, G., “Distribution of neutrals scattered off a wall”, PPPL Appl. Phys. Rep. No. 1, PPPL (1980)

[43] LOARER, T., et al., “Comparison of long term fuel retention in JET between carbon and the ITER-Like Wall”, Journal of Nuclear Materials 438 S108 (2013)

[44] BREZINSEK, S., et al. “Fuel retention studies with the ITER-Like Wall in JET”, Nuclear Fusion 53 083023 (2013)

"*JINTRAC was used under licence agreement between Euratom and CCFE, Ref. Ares(2014)3576010 - 28/10/2014. This work was funded jointly by the RCUK Energy Programme [grant number EP/I501045] and by ITER Task Agreement C19TD51FE implemented by Fusion for Energy under Grant GRT-502. To obtain further information on the data and models underlying this paper, whose release may be subject to commercial restrictions, please contact PublicationsManager@ccfe.ac.uk. The views and opinions expressed do not necessarily reflect those of Fusion for Energy which is not liable for any use that may be made of the information contained herein. The views and opinions expressed herein do not necessarily reflect those of the ITER Organization.*